Title: SARS-CoV-2 Viral Clearance and Evolution Varies by Extent of Immunodeficiency

Authors: Yijia Li[*1 2 3] , Manish C. Choudhary[*1] , James Regan[*1] , Julie Boucau[4] , Anusha Nathan[4 5] , Tessa Speidel[6] , May Yee Liew[2 7] , Gregory E. Edelstein[1] , Yumeko Kawano[1] , Rockib Uddin[2 7] , Rinki Deo[1] , Caitlin Marino[4] , Matthew A. Getz[4], Zahra Reynold[2] , Mamadou Barry[2] , Rebecca F. Gilbert[2] , Dessie Tien[2] , Shruti Sagar[2] , Tammy D. Vyas[2] , James P. Flynn[1] , Sarah P. Hammond[2] , Lewis A. Novack[1], Bina Choi[1], Manuela Cernadas[1], Zachary S. Wallace[2] , Jeffrey A. Sparks[1] , Jatin M. Vyas[2 4] , Michael S. Seaman[6] , Gaurav D. Gaiha[2 4] , Mark J. Siedner[#2] , Amy K. Barczak[#2 4] , Jacob E. Lemieux[#2 7] , Jonathan Z. Li[#1]

Affiliations:

1. Department of Medicine, Brigham and Women's Hospital, Harvard Medical School, Boston, MA, USA
2. Department of Medicine, Massachusetts General Hospital, Harvard Medical School, Boston, MA, USA
3. University of Pittsburgh Medical Center, Pittsburgh, PA, USA
4. Ragon Institute of MGH, MIT and Harvard, Cambridge, MA, USA
5. Program in Health Sciences and Technology, Harvard Medical School and Massachusetts Institute of Technology, Boston, MA 02115, USA
6. Center for Virology and Vaccine Research, Beth Israel Deaconess Medical Center, Harvard Medical School, Boston, MA, USA
7. Broad Institute of MIT and Harvard, Cambridge, MA, USA

*, # Equal contribution

Abstract

Despite vaccination and antiviral therapies, immunocompromised individuals are at risk for prolonged SARS-CoV-2 infection, but the immune defects that predispose to persistent COVID-19 remain incompletely understood. In this study, we performed detailed viro-immunologic analyses of a prospective cohort of participants with COVID-19. The median time to nasal viral RNA and culture clearance in the severe hematologic malignancy/transplant group (S-HT) were 72 and 40 days, respectively, which were significantly longer than clearance rates in the severe autoimmune/B-cell deficient (S-A), non-severe, and non-immunocompromised groups ($P<0.001$). Participants who were severely immunocompromised had greater SARS-CoV-2 evolution and a higher risk of developing antiviral treatment resistance. Both S-HT and S-A participants had diminished SARS-CoV-2-specific humoral, while only the S-HT group had reduced T cell-mediated responses. This highlights the varied risk of persistent COVID-19 across immunosuppressive conditions and suggests that suppression of both B and T cell responses results in the highest contributing risk of persistent infection.

Main Text

Introduction

Coronavirus Disease 2019 (COVID-19) vaccinations have drastically transformed the landscape of the COVID-19 pandemic by offering significant protection against infection acquisition, and severe diseases(*1, 2*), and ultimately have averted tens of millions of deaths(*3*). Unfortunately, not all individuals respond to vaccination equally well, and immunocompromised individuals can have poor vaccine responses(*4, 5*) and worse COVID-19-related outcomes(*6, 7*). Each new variant of Severe Acute Respiratory Syndrome Coronavirus-2 (SARS-CoV-2) brings risks of resistance to current treatments, particularly targeted antibody therapies(*8, 9*), resistance to vaccine-induced and naturally acquired immunity(*9, 10*), and increased transmissibility(*10*). Immunocompromised individuals have been observed to harbor detectable SARS-CoV-2 virus for longer than non-immunocompromised individuals(*11-13*). Such individuals represent a potential origin of novel SARS-CoV-2 variants as persistent infection has been associated with accelerated viral evolution(*11, 13*). However, the immunocompromised state is composed of a range of conditions and immune defects. These defects that predispose to persistent COVID-19 remain under-characterized. While there have been a number of case reports of persistent COVID-19 in immunosuppressed individuals(*11-16*) showing excessively prolonged viral shedding, persistent disease, and intra-host virological genetic diversity, there remains a need for larger scale studies with a comprehensive virologic and immunologic characterization to better elucidate the immunologic risk factors for and mechanisms of persistent infection. To this end, we hereby present a detailed longitudinal virological and immunological analysis of a cohort of immunocompromised and non-immunocompromised participants with SARS-CoV-2 infection with the goal of characterizing the virologic spectrum of persistent infection and exploring the immunologic determinants that predispose to its occurrence.

63 ## Results

64 ### Participant Characteristics

65 Fifty-six immunocompromised participants and 184 non-immunocompromised participants
66 enrolled in the POSITIVES longitudinal cohort study were included in this analysis (*17-19*).
67 Demographic information and key viral characteristics are shown in Table 1.
68 Immunocompromised participants were significantly older than non-immunocompromised
69 controls (median 55 vs 46 years, P=0.001), and more likely to receive monoclonal antibody
70 (mAb) and/or antiviral treatment against SARS-CoV-2. The two groups had comparable sex,
71 race, and ethnicity profiles and a similar median time from symptom onset/first positive COVID-
72 19 test to enrollment (5 vs 4 days). We further subdivided immunocompromised participants into
73 the severe hematologic-oncology/transplant (S-HT, n=12), severe autoimmune/B-cell deficient
74 (S-A, n=13) and non-severe (NS, n=31) groups (refer to Supplementary Tables 1 and 2 for
75 detailed categorization). Three participants died due to severe COVID-19 or COVID-19 related
76 complications, all of whom were in the immunocompromised sub-group (S-HT and S-A).
77

78 ### Delayed Viral Clearance in Hematologic Oncology and Transplant Participants

79 We first aimed to characterize viral dynamics in the upper respiratory tract in participants with
80 different categories of immunocompromising conditions. Immunocompromised and non-
81 immunocompromised participants had similar peak vRNA levels (5.1, 5.1, 4.9, and 5.7 $\log_{10}$
82 SARS-CoV-2 copies/ml in S-HT, S-A, NS and non-immunocompromised groups, P=0.5).
83 However, the rates of nasal vRNA decay were significantly different between the
84 immunocompromising categories, with the S-HT group demonstrating significantly slower viral
85 clearance compared to other groups (Fig. 1a and 1b). Median time to nasal vRNA clearance in
86 the S-HT group was 72 days (95% confidence interval [CI] 5, not available [NA]) compared to 7
87 (6, NA) days for the S-A, 11 (8, 16) days for the NS and 11 (10, 12) days for the non-
88 immunocompromised group (Fig. 1b, Log-rank P=0.002). Similarly, the S-HT group experienced

89 a significant delay in the clearance of culturable virus (Fig. 1c and 1d). Median time to viral
90 culture clearance in the S-HT group was 40 days (95%CI 5, NA) compared to 6.5 (5, NA) days
91 for the S-A group, 6 days (5, 7) for the NS group and 7 days (6, 7) for the non-
92 immunocompromised group (Fig. 1d, log-rank P<0.001, Fig. 1d). After 30 days from symptom
93 onset or first positive test, 50%, 15%, and 6.5% of participants from S-HT, S-A and NS groups
94 had detectable vRNA, compared to 0% in non-immunocompromised group (P<0.0001,
95 Supplementary Fig. 1a). In addition, 50% of S-HT and 8.3% of S-A participants still had
96 culturable virus, compared to 0% in the NS and non-immunocompromised groups after 30 days
97 (P<0.0001, Supplementary Fig. 1b). Compared to the non-immunocompromised group, the S-
98 HT group was significantly associated with delayed vRNA clearance (adjusted hazard ratio
99 [aHR] for viral clearance, 0.32, 95%CI 0.12-0.83, P=0.02) and culturable virus clearance (aHR
100 0. 27 for viral clearance, 95% CI 0.12-0.63, P=0.002), after adjusting for demographics, number
101 of vaccinations and antiviral use (Table 2).
102
103 **Increased Viral Evolution and Genetic Diversity in Immunocompromised Participants**
104 We used gene-specific next-generation sequencing approach to quantify the number of unique
105 intra-host single-nucleotide variants (iSNVs) in the S gene present at >3% frequency within
106 each sample. This analysis was limited to participants with a viral genome available both at
107 baseline and at least one follow-up timepoint. Severely immunocompromised (S-HT and S-A)
108 participants harbored a greater number of iSNVs over time compared to NS and non-
109 immunocompromised group participants, although these comparisons did not reach statistic
110 significance (Fig. 2a). To evaluate viral diversity, we calculated the average pairwise distance
111 both at the nucleotide and at the amino-acid level. Nucleotide average pairwise distance was
112 significantly higher in the severe immunocompromised (S-HT and S-A) group compared to
113 either non-severe (4.0E-4 vs 8.2E-5, P<0.001 Dunn's test with Benjamini-Hochberg adjustment)
114 or non-immunocompromised groups (4.0E-4 vs 2.3E-5, P<0.001, Fig. 2b). Similar results were

115 obtained when the average pairwise distances were calculated for amino acids (Supplementary
116 Fig. 2a). Among participants with longitudinal sequences, 39% of the participants in
117 immunocompromised group versus 12% in the non-immunocompromised group had evidence
118 of viral nucleotide changes (Fisher's exact P<0.001, Fig. 2c). These nucleotide changes were
119 distributed across the entire length of the S gene (Fig. 2d).
120

121 **Increased Risk of Treatment-Emergent Resistance to Anti-SARS-CoV-2 Monoclonal**
122 **Antibody Therapy**

123 Deep sequencing analysis of Spike gene was carried out to evaluate the dynamics of mutation
124 emergence in the presence of mAb treatment as earlier reports have shown evidence of mAb
125 resistance emergence both in immunocompromised and non-immunocompromised
126 participants(*13, 20-29*). In total, 34 participants across different study groups received mAb
127 therapy, 10 in S-HT, 9 in S-A, 5 in NS, and 10 in non-immunocompromised groups (Details in
128 Supplementary Table 3). Of these, we were able to evaluate the risk of resistance emergence in
129 a subset of participants for whom sequences were available at both baseline and at least one
130 follow-up time point. Five out of nine (56%) severely immunocompromised participants (S-HT
131 and S-A) developed mAb-specific resistance mutations (Supplementary Fig. 2b). This was a
132 significantly higher rate than that found in the non-severe or non-immunocompromised groups
133 (0/11 [0%] combined, Fisher's exact P=0.008) (Fig 2e).
134

135 **Suboptimal Humoral Response in Severely Immunocompromised Participants**

136 We next characterized the antibody response in immunocompromised and non-
137 immunocompromised participants. In participants whose serum sample was available (n=94),
138 including those who had previously received monoclonal antibodies, we found no significant
139 difference in nAb titers between the different immunocompromised and non-
140 immunocompromised groups at early and later sampling time points, although this analysis may

141 have been limited due to individuals who received anti-SARS-CoV-2 monoclonal antibody
142 infusion before sample collection (either therapeutic or pre-exposure prophylaxis) (Fig. 3a and
143 3b). The non-immunocompromised group had a significant increase in anti-ancestral and anti-
144 variant spike nAb levels during follow-up, whereas we did not observe a significant increase in
145 antibody levels in the immunocompromised group (Fig. 3a and 3b). However, after excluding
146 individuals with exposure to mAb therapies, the severe immunocompromised group showed no
147 significant changes in either anti-ancestral or anti-variant Spike nAb levels, while the non-severe
148 immunocompromised group demonstrated a moderate increase and the non-
149 immunocompromised group demonstrated the greatest increase in nAb levels, plateauing at day
150 25-30 (Fig. 3c and d).
151
152 In a generalized estimating equation (GEE) model adjusted for factors associated with nAb
153 levels, severely immunocompromised participants were only able to mount 0.18-fold
154 (approximately 5-fold lower) of the anti-ancestral Spike antibody (95% CI 0.05-0.60) and 0.08-
155 fold (approximately 12-fold lower) of the anti-variant Spike antibody (95% CI 0.03-0.22)
156 compared to non-immunocompromised participants (Supplementary Fig. 3a, b). Non-severe
157 immunocompromised status was not associated with significant differences in nAb changes
158 from acute to post-infection, compared to non-immunocompromised group. In the whole cohort,
159 each dose of vaccinations prior to SARS-CoV-2 infection was associated with 1.70-fold (95% CI
160 1.25 to 2.30) and 1.35-fold (95% CI 1.01 to 1.79) increase in anti-ancestral and anti-variant
161 Spike antibody levels, respectively (Supplementary Fig. 3ab).
162
163 We also evaluated binding antibody against nucleocapsid protein because this assay is not
164 affected by monoclonal antibody use. Similar to nAb, individuals in the S-HT and S-A sub-
165 groups had significantly blunted increases in nucleocapsid binding Ab development from acute
166 to post-infection, and significantly lower binding Ab levels compared to NS and non-

167 immunocompromised groups (Fig. 3e). Longitudinally, binding Ab levels in NS and non-
168 immunocompromised groups plateaued around day 20-25 at a level of 1-1.5 $\log_{10}$ IU/ml, while
169 S-HT/S-A groups exhibited delayed development to a level below 1 $\log_{10}$ IU/ml after day 50 (Fig.
170 3f).
171
172 **T Cell Responses**
173 In a recent study, Apostolidis et al. demonstrated elevated spike-specific $CD8^+$ T cell responses
174 in COVID-19 mRNA vaccinated participants with multiple sclerosis receiving anti-CD20
175 treatment compared to healthy controls(*30*). However, it remains largely unknown if different
176 types and levels of immunosuppression are associated with a similar T cell immunophenotype.
177 To this end, we profiled the T cell effector function using enzyme-linked immunosorbent spot
178 (ELISpot) and antigen-specific proliferation assay for a selected group of participants based on
179 sample availability. The non-immunocompromised group had lower interferon gamma (IFN-γ)
180 producing units per million cells upon stimulation at both blood draws (acute infection 0-14 days,
181 and post-acute 15-60 days after symptom onset or first positive COVID-19 test) compared to
182 both NS and S-A groups in response to both ancestral and variant-specific Spike peptide pools
183 (Fig. 4a). Individuals in the S-A group tended to have the highest levels of CD4+ and $CD8^+$ T
184 cell proliferation upon spike peptide pool stimulation, especially compared to the S-HT and non-
185 immunocompromised individuals (Fig. 4bc and Supplementary Fig. 4). In longitudinal analysis,
186 the S-HT group showed poor functional $CD4^+$ and $CD8^+$ T cell proliferation, despite a
187 comparable IFN-γ secretion level compared to the non-immunocompromised group (Fig. 4d). In
188 contrast, the S-A group showed robust T cell proliferation over time, in response to both
189 ancestral and variant-specific spike peptide pools compared to all other groups, suggestive of
190 either an antigen-stimulated compensatory effect in the setting of B cell deficiency or a
191 medication-related T cell priming.

192 **Discussion**

193 Understanding viral and immune control characteristics of COVID-19 infection is crucial to our
194 ability to care for immunocompromised individuals at greatest risk of persistent and severe
195 infection. Moreover, it can guide public health interventions and shed light on vaccine
196 development that protects immunocompromised individuals. In this study, we performed an in-
197 depth virologic and immunologic evaluation of a cohort of immunocompromised and non-
198 immunocompromised individuals. We demonstrated a hierarchy of immunocompromised
199 conditions that increase the risk of delayed viral clearance and SARS-CoV-2 evolution.
200 Furthermore, we identified the varied risk of persistent COVID-19 across immunosuppressive
201 conditions and suppression of both B and T cell responses in those at the highest risk of
202 persistent infection. Specifically, we found that individuals with a history of hematological
203 malignancy and organ transplant demonstrated the greatest delay in viral clearance that may be
204 mediated by suppression of both the B and T cell responses. In contrast, those with B cell
205 immunodeficiency had an intermediate risk of chronic infection in the setting of an immune
206 response showing compensatory heightened levels of SARS-CoV-2-specific T cell function.
207

208 Our cohort study confirmed findings from prior case reports and case series. In a review by
209 Dioverti et al., the authors summarized cases of persistent COVID-19 lasting from
210 approximately one month to one year(*31*). These included a spectrum of immunocompromised
211 hosts from individuals with solid organ transplants, hematological malignancy(*14, 20, 22, 23, 25,*
212 *29, 32-36*), and autoimmune diseases receiving immunosuppressive therapies. However,
213 immunocompromise is a broad spectrum and, until now it has not been clear which
214 immunosuppressive conditions represent the greatest risk for persistent infection. The results of
215 our study provide critical insight as to the hierarchy of risk for delayed SARS-CoV-2 RNA and
216 culture clearance, and viral evolution. Specifically, we found that demonstrated that individuals
217 with solid organ transplant and hematological malignancy are associated with the longest period

218 of viral RNA and culturable viral shedding, followed by severely immunocompromised
219 participants with autoimmune conditions receiving B-cell depleted therapy and/or those with B
220 cell deficiency. Participants with mild non-severe immunocompromise, such as those with
221 autoimmune diseases receiving anti-tumor necrosis factor (TNF) treatment, had similar viral
222 shedding dynamics to non-immunocompromised participants.
223
224 There have been several prior case reports of immunosuppressed individuals with chronic
225 COVID-19 and accumulation of viral polymorphisms and drug resistance mutations(*13, 14, 21,*
226 *27, 34*), but there has been little in the way of more systematic evaluation of viral evolution. In
227 this study, we used S gene-specific deep sequencing to assess longitudinal viral evolution and
228 diversity. Our results show that severe immunosuppression is associated with increased viral
229 evolution and diversification. In addition, severe immunocompromised hosts had a greater risk
230 of developing treatment-emergent resistance mutations to mAb therapy when compared to non-
231 immunocompromised group participants. These findings highlight the potential for
232 immunocompromised individuals to serve as a source for SARS-CoV-2 evolution and drug
233 resistance, consistent with isolated reports of immunocompromised hosts implicated in the
234 emergence of highly mutated SARS-CoV-2 variants(*13, 15, 16, 24, 28, 37-40*). It should be
235 noted though that even within the category of severe immunocompromise, participants
236 demonstrated a range of viral diversification and evolution patterns, and additional studies are
237 needed to fully assess the drivers of accelerated viral evolution.
238
239 Another highlight of our study is our use of in-depth analysis of B and T cell responses,
240 including SARS-CoV-2-specific neutralizing and binding antibody levels, as well as ELISpot and
241 T cell proliferation studies. We noted lower levels of neutralizing antibody against both ancestral
242 virus and variant virus in the severe immunocompromised group (less than 10-20% compared
243 to non-immunocompromised individuals), after adjusting for vaccination doses, monoclonal

244 antibody use, and demographic confounders. Each additional dose of vaccination is associated
245 with an approximately 1.5-fold increase in antibody levels in the whole cohort, underscoring the
246 importance of adherence to COVID-19 vaccination recommendations. However, there is
247 evidence that non-B-cell immunity may be sufficient for the clearance of SARS-CoV-2. Early in
248 the pandemic, cases were reported of individuals with X-linked agammaglobulinemia who
249 developed COVID-19 pneumonia, but subsequently recovered despite a lack of SARS-CoV-2-
250 specific immunoglobulins(*41*). In our study, the risk of chronic infection was highest in S-HT
251 participants. This group of participants was found to have both suboptimal humoral and cell-
252 mediated immune responses. The “near-normal” level of effector ELISpot responses in S-HT
253 individuals, compared to the non-immunocompromised group, is the likely the result of exposure
254 to high levels of SARS-CoV-2 antigen, while the reduced proliferation demonstrates
255 compromised functionality. In contrast, the S-A participants had an even more robust SARS-
256 CoV-2-specific proliferative T-cell responses than the non-immunocompromised group,
257 indicating increased levels of functional SARS-CoV-2-specific $CD8^+$ T cell responses, which
258 was associated with an intermediate risk of chronic infection. These results align with some
259 intriguing reports that individuals receiving anti-CD20 treatment may demonstrate a stronger T-
260 cell responses, in particular more robust activation-induced marker-positive $CD8^+$ T cell
261 responses(*30*). We found that both $CD8^+$ T cell response and $CD4^+$ T-cell responses, including
262 proliferation in response to both ancestral and variant-specific spike peptides, were more
263 pronounced in S-A group compared to other non-immunocompromised groups. Together with
264 the results from Apostolidis et al.(*30*), our results raise the question of whether individuals with B
265 cell deficiencies may have a lower risk of persistent SARS-CoV-2 infection due to preserved T
266 cell function, either as a compensatory mechanism or T cell priming by certain B cell-depleting
267 therapies.
268

269 There are several limitations to this study. We included a relatively small number of individuals
270 with malignant hematological conditions or transplant history, and we were able to obtain blood
271 samples from only a subset of the participants to characterize their humoral and T-cell immunity.
272 Larger studies are needed to provide greater precision as to extent of immune defect or
273 immunosuppressive medication that may place patients at the greatest risk of chronic infection
274 and viral evolution. We also did not analyze markers reflecting innate immunity, including
275 soluble inflammatory markers and monocyte phenotypes. Our study focused on virologic and
276 immunologic responses after COVID-19 and it is unclear how these may contribute to
277 persistence and severity of symptoms. Furthermore, we only evaluated Spike-specific humoral
278 and cellular immunity, while immunity targeting other structural or non-structural proteins has
279 been shown to alter disease course(*42, 43*).
280
281 In conclusion, in this prospective cohort of well-characterized individuals with acute COVID-19,
282 we demonstrated a correlation between a hierarchy of immunocompromised conditions and
283 SARS-CoV-2 viral shedding, viral evolution, and adaptive immunity. Our results highlight the
284 finding that the risk of chronic SARS-CoV-2 infection is not uniform across immunosuppressive
285 conditions and provide clarity on which immunosuppression conditions predispose to delayed
286 SARS-CoV-2 RNA and culture clearance, and viral evolution. The high risk populations
287 identified in this study may benefit from targeted public health and additional therapeutic
288 interventions. In addition, the results provide further insights on the humoral and cell-mediated
289 immune correlates of viral clearance, which is crucial for the development of improved vaccines
290 and future therapies.

291 ## Materials and Methods

292 ### Participant Enrollment and Sample Collection

293 We enrolled participants with a positive COVID-19 test in the Mass General Brigham Medical
294 HealthCare System as part of the POSt-VaccInaTIon Viral CharactEristics Study (POSITIVES)
295 (*17, 19*) in addition to one immunocompromised participant from our previous study. Each
296 participant's medical record was reviewed for demographic data, immunosuppression status,
297 and COVID-19 treatment history by board-certified clinicians. For the POSITIVES study,
298 participants self-collected anterior nasal swabs every 2-3 days to a total of 6 samples over 2
299 weeks. Participants with immunocompromised conditions were offered to collect additional
300 swabs when possible and were followed until they had two consecutive negative PCR tests. For
301 this one immunocompromised participants reported previously(*13*), nasopharyngeal swab was
302 collected by healthcare providers. In a subset of participants who agreed to provide blood
303 sample, the first blood draw was done generally before day 15 of symptom onset (acute phase)
304 or first positive PCR or antigen test for COVID-19, and second blood draw between 15-60 days
305 after (post-acute phase) (Supplementary Fig. 5). This study was approved by Mass General
306 Brigham Institutional Review Board and all participants have signed informed consent upon
307 entry to the study.

308

309 ### Categorization for Immunocompromised Conditions

310 Immunocompromised participants were further categorized into the following groups: severe
311 immunocompromised participants, which were further categorized into severe-hematological
312 malignancy/transplant patients (S-HT), severe autoimmune patients (S-A, participants with
313 autoimmune condition receiving B-cell targeting agents or B cell deficiency); and non-severe
314 immunocompromised participants (NS). This categorization was based on a recent cohort study
315 which demonstrated a hierarchy of antibody response to COVID-19 vaccinations in different
316 medical conditions(*4, 44*). Detailed classification criteria were listed in Supplementary Table 1.

317

318 **SARS-CoV-2 Viral Load Assay**

319 SARS-CoV-2 viral RNA (vRNA) were quantified as described previously(*45*). Briefly, virions
320 were pelleted from nasal swab fluid by centrifugation at 21,000g for 2 hours at 4°C. Trizol-LS
321 Reagent (Thermo fisher Scientific, Waltham, MA) was added to the pellet, vortexed, and
322 incubated on ice for 10 minutes. Chloroform was added and the solution was vortexed before
323 centrifugation at 21,000g for 15 minutes at 4°C. RNA was isolated from the aqueous layer by
324 isopropanol precipitation and eluted in DEPC-Treated water (Thermo fisher Scientific, Waltham,
325 MA). SARS-CoV-2 RNA copies were quantified with an in-house viral load assay using the CDC
326 2019-nCoV_N1 primer and probe set (Integrated DNA Technologies, Coralville, IA). The
327 efficiency of the RNA extraction and RT-qPCR amplification was evaluated by quantifying the
328 RCAS RNA recovered from each sample and the two N1 controls. The importin-8 (IPO8) human
329 housekeeping gene was also amplified and evaluated as a measure of sample collection
330 quality. Samples were run in triplicate wells for N1, and in duplicate wells for RCAS and IPO8.

331

332 **SARS-CoV-2 Viral Culture Assay**

333 Viral culture was performed as previously reported(*17*). Vero-E6 cells (ATCC, Manassas, VA)
334 maintained in DMEM (Corning, Corning, NY) supplemented with HEPES (Corning, Corning,
335 NY), 1X Penicillin (100 IU/mL)/Streptomycin (100 µg/ml) (Corning, Corning, NY), 1X Glutamine
336 (Glutamax, Thermo fisher Scientific, Waltham, MA) and 10% FBS (MilliporeSigma, Burlington,
337 MA) were plated 16-20 hours before infection. Each sample consisting of nasal swab fluid was
338 thawed on ice and filtered through a Spin-X 0.45 um filter (Corning, Corning, NY) at 10,000 xg
339 for 5 minutes. Before infection the media was changed to DMEM supplemented with HEPES,
340 1X Antibiotic/Antimycotic (Thermo Fisher, Waltham, MA), 1X Glutamine, 2% FBS and 5 µg/mL
341 of polybrene (Santa Cruz Biotechnologies, Dallas, TX). Each filtered sample was then used to

342 inoculate Vero-E6 cells by spinfection (2,000x g for 1 hour at 37C). Each condition was plated in
343 quadruplicate wells in 1:5 dilutions across half the plate. The plates were observed at 7-days
344 post-infection using a light microscope to check for cytopathogenic effect (CPE) and a median
345 tissue culture infectious dose ($TCID_{50}$) was calculated for each sample.
346
347 **Neutralizing Antibody Responses**
348 Neutralizing activity against SARS-CoV-2 pseudovirus was measured using a single-round
349 infection assay in 293T/ACE2 target cells(*18*). Pseudotyped virus particles were produced in
350 293T/17 cells (ATCC, Manassas, VA) by co-transfection of plasmids encoding codon-optimized
351 full-length Spike (ancestral-D614G, Delta, Omicron-BA.1, Omicron-BA.2, Omicron-BA.4/5),
352 packaging plasmid pCMV ΔR8.2, and luciferase reporter plasmid pHR' CMV-Luc. Packaging
353 and luciferase plasmids were kindly provided by Dr. Barney Graham (NIH, Vaccine Research
354 Center). The 293T cell line stably overexpressing the human ACE2 cell surface receptor protein
355 was kindly provided by Drs. Michael Farzan and Huihui Ma (The Scripps Research Institute).
356 For neutralization assays, serial dilutions of patient sera were performed in duplicate followed by
357 addition of pseudovirus. Pooled serum samples from convalescent COVID-19 patients or pre-
358 pandemic normal healthy serum (NHS) were used as positive and negative controls,
359 respectively. Plates were incubated for 1 hour at 37℃ followed by addition of 293/ACE2 target
360 cells ($1x10^4$/well). Wells containing cells + pseudovirus (without sample) or cells alone acted as
361 positive and negative infection controls, respectively. Assays were harvested on day 3 using
362 Promega BrightGlo luciferase reagent and luminescence detected with a Promega GloMax
363 luminometer (Promega, Madison, WI). Titers are reported as the dilution of serum that inhibited
364 50% virus infection (ID_{50} titer). Pseudovirus-based neutralization assays were conducted using
365 ancestral Spike protein, as well as Delta- and Omicron- (BA.1, BA.2, or BA.4/5) Spike. Anti-
366 variant neutralizing antibody level (nAb) was determined based on the viral strain each

367 participant was infected with (either by sequencing or in small proportion, imputed by time of
368 infection when specific strain was prevalent).
369
370 **Nucleocapsid binding antibody assay**
371 Binding antibody against Nucleocapsid protein was measured using Coronavirus Ig Total
372 Human 11-Plex ProcartaPlex™ Panel (Thermo fisher Scientific, Waltham, MA) according to the
373 manufacturer's instruction.
374
375 **T Cell Enzyme-linked immunosorbent spot (ELISpot) Assay**
376 Interferon (IFN)-γ ELISpot assay was reported in our previous study and were performed
377 according to the manufacturer's instructions (Mabtech, Cincinnati, OH)(*46*). Briefly, peripheral
378 blood mononuclear cells (PBMCs) were incubated with SARS-CoV-2 peptide pools (MGH
379 Peptide Core) at a final concentration of 0.5μg/ ml for 16–18h (100,000-200,000 cells per test).
380 Anti-CD3 (Clone OKT3, Biolegend, 0.5μg/mL, San Diego, CA) and anti-CD28 Ab (Clone
381 CD28.2, Biolegend, 0.5μg/mL, San Diego, CA) were used as positive controls. To quantify
382 antigen-specific responses, mean spots of the DMSO negative control wells were subtracted
383 from the positive wells. The results were expressed as spot-forming units (SFU) per 10^6
384 PBMCs. Responses were considered positive if the results were >5 SFU/10^6 PBMCs following
385 control subtraction. If negative DMSO control wells had >30 SFU/10^6 PBMCs or if positive
386 control wells (anti-CD3/anti-CD28 stimulation) did not have >1000 spot-forming units, the results
387 were deemed invalid and excluded from further analysis.
388
389 **T Cell Proliferation Assay**
390 T Cell proliferation assay was reported previously(*46*). Briefly, PBMCs were incubated in PBS
391 with 0.5 uM carboxyfluorescein succinimidyl ester (CFSE; Life Technologies, Carlsbad, CA) or
392 CellTrace™ Far Red (CTFR, Invitrogen, Waltham, MA) at 37°C for 20 min. Then they were

393 washed and resuspended at 0.5-1 × 10^6/mL and plated into 96-well U-bottom plates (Corning) in
394 200 µL of. media. Peptide pools were added at a final concentration of 0.5 µg/mL, followed by
395 incubation at 37°C, 5% CO_2 for six days. The PBMC staining antibody panels are in
396 Supplementary Materials. Cells were washed and fixed in 2% paraformaldehyde prior to flow
397 cytometric analysis on a BD LSR II (BD Biosciences, Franklin Lakes, NJ). A positive
398 proliferation response was defined as a percentage of $CD3^+CD4^+$ or $CD3^+CD8^+$ $CFSE^{low}$ or
399 $CTFR^{low}$ cells with at least 1.5x greater than the highest of two negative-control wells and
400 greater than 0.2% $CFSE^{low}$ or $CTFR^{low}$ cells in magnitude following background subtraction.
401

402 **SARS-CoV-2 S-gene Sequencing**

403 SARS-CoV-2 viral RNA (vRNA) isolation as described previously(*45*). RNA was converted to
404 cDNA using Superscript IV reverse transcriptase (Invitrogen, Waltham, MA) as per manufacturer's
405 instructions). Spike (S) gene amplification was performed using a nested PCR strategy with in-
406 house designed primer sets targeting codons 1–814 of the Spike as previously described(*28*).
407 Further, PCR products from different individuals were pooled, and Illumina library construction
408 was performed using the Nextera XT library prep kit (Illumina). Sequencing was performed on the
409 Illumina MiSeq platform and deep sequencing data analysis was carried out using the Stanford
410 Coronavirus Antiviral & Resistance Database (CoVDB) platform
411 (https://covdb.stanford.edu/sierra/sars2/by-reads/?cutoff=0.01&mixrate=0.01)(*47*). Input FASTQ
412 sequence alignment with Wuhan-Hu-1 reference was done using MiniMap2 version 2.22 in
413 CodFreq pipeline (https://github.com/hivdb/codfreq). The output of MiniMap2, an aligned SAM
414 file, is converted to a CodFreq file by an in-house written Python script using a PySam library
415 (version: 0.18.0) and further analyzed with the CoVDB. PCR and sequencing runs were
416 performed once with the appropriate positive and negative controls. For S gene analysis, amino
417 acid variants were then called at the codon level using perl code and used for resistance
418 interpretation with a 1% limit of detection. The accuracy of the deep sequencing platforms was

419 evaluated with a control library of clonal SARS-CoV-2 sequences mixed at known concentrations
420 as described previously(*48*). Mutations detected by next-generation sequencing at <20% of the
421 viral population were labelled as 'low-frequency' variants as they would largely be missed by
422 traditional Sanger sequencing. A minimum average of 500x sequencing coverage per sample
423 was required for variant calling. SARS-COV-2 variant calling was done using 3 different variant
424 calling platforms, namely, CoVDB(*47*), Scorpio call v1.2.123 (https://pangolin.cog-uk.io/), and
425 Nextclade v.1.13.2 (https://clades.nextstrain.org/)(*49*).
426
427 **Single nucleotide variation, and genetic diversity analysis**
428 For assessing intrahost single nucleotide variation (iSNV), data from only those participants were
429 included for whom sequence data from baseline and at least one follow-up time point were
430 available. SNV analysis was performed using PASeq SARS-CoV-2 pipeline (www.paseq.org).
431 Briefly, raw sequence files were quality filtered and adapter-trimmed using trimmomatic (v0.30).
432 Contaminating sequences were filtered out using BBMap Suite (v35.76). Duplicated reads were
433 detected using fastuniq (v1.1). High quality non-redundant reads were then aligned to SARS-
434 CoV-2 Wuhan reference (NC_045512.2) using Bowtie2 (v.2.3.2). Resulting alignments were
435 processed with samtools (v.1.2) and iVar (v1.4.2) to obtain nucleotide variant VCF files.
436 Nucleotide variants present at 100% frequency of the total viral population at all time points
437 indicative of lineage defining mutations were excluded from the iSNV analysis. Genetic diversity
438 between multiple sequences of an individual were assessed by average pairwise distance in
439 MEGA both at the nucleotide and amino-acid level.
440
441 **Statistical Analysis**
442 Categorical variables were summarized using total number and percentage and between-group
443 differences were evaluated using either chi-squared test or Fisher's exact test when
444 appropriate. Continuous variables were summarized with median and interquartile ranges and

compared with non-parametric methods (Wilcoxon rank-sum test to compare two groups and Dunn's test with Benjamini-Hochberg adjustment to compare three or more groups). Within group comparison was conducted using paired Wilcoxon signed-rank test without adjustment for multiple comparisons. We also used generalized estimating equation (GEE) with Gaussian estimation to evaluate between-group differences accounting for repeated measurement during longitudinal follow-up. R (4.3.0) was used for statistical analyses. Two-tailed tests were used for all the analyses and $P<0.05$ was considered statistically significant unless specified otherwise.

List of Supplementary Materials

Supplementary Methods

Supplementary Tables 1-3

Supplementary Figures 1-5

Acknowledgements

We thank all the participants for their participation in this important study. We thank all the healthcare workers who take care of them and kindly refer them to the POSITIVES study. This work was supported by the National Institutes of Health (U19 AI110818), the Massachusetts Consortium for Pathogen Readiness SARS-CoV-2 Variants Program and the Massachusetts General Hospital Department of Medicine. Drs. JA Sparks and ZS Wallace are supported by the National Institute of Arthritis and Musculoskeletal and Skin Diseases (R01 AR080659). Dr. JA Sparks is also supported by the Llura Gund Award funded by the Gordon and Llura Gund Foundation. Dr. GD Gaiha is supported by the NIH (DP2AI154421, R01AI176533 and DP1DA058476), the Bill and Melinda Gates Foundation, Burroughs Wellcome Career Award for Medical Scientists and Howard Goodman Fellowship. Dr. JZ Li was also supported by a grant from Merck. Dr. Y Li was supported by Rustbelt CFAR (Case Western Reserve University/University Hospitals Cleveland Medical Center and University of Pittsburgh, P30 AI036219). The BSL3 laboratory where viral culture work was performed is supported by the Harvard CFAR (P30 AI060354). The funders had no role in the study design; in the collection, analysis, and interpretation of data; in the writing of the manuscript; or in the decision to submit the manuscript for publication.

Authors Contribution

Study conceptualization: MJ Siedner, AK Barczak, JE Lemieux, JZ Li

First draft writing: Y Li, MC Choudhary, J Regan, JZ Li

Draft review, discussion and approval: All authors

Statistical analyses: Y Li, MC Choudhary, R Deo, J Regan

Chart review and participant classification: Y Li, Y Kawano, ZS Wallace, JA Sparks

Virology assays: J Regan, J Boucau, GE Edelstein, C Marino, JP Flynn

Sequencing analyses: MC Choudhary, R Uddin, R Deo, JE Lemieux, JZ Li

Neutralizing antibody assays: T Speidel, MS Seaman

Binding antibody assays: MY Liew

T cell assays: A Nathan, MA Getz, GD Gaiha

Study coordination, sample collection, participant referral: Z Reynold, M Barry, RF Gilbert, D Tien, S Sagar, TD Vyas, SP Hammond, LA Novack, B Choi, M Cernadas, ZS Wallace, JA Sparks, JM Vyas

Database management: MJ Siedner, RF Gilbert

491 **References**

492 1. H. M. El Sahly *et al.*, Efficacy of the mRNA-1273 SARS-CoV-2 Vaccine at Completion of
493 Blinded Phase. *N Engl J Med* **385**, 1774-1785 (2021).
494 2. E. D. Moreira, Jr. *et al.*, Safety and Efficacy of a Third Dose of BNT162b2 Covid-19
495 Vaccine. *N Engl J Med* **386**, 1910-1921 (2022).
496 3. O. J. Watson *et al.*, Global impact of the first year of COVID-19 vaccination: a
497 mathematical modelling study. *Lancet Infect Dis* **22**, 1293-1302 (2022).
498 4. G. Haidar *et al.*, Prospective Evaluation of Coronavirus Disease 2019 (COVID-19)
499 Vaccine Responses Across a Broad Spectrum of Immunocompromising Conditions: the
500 COVID-19 Vaccination in the Immunocompromised Study (COVICS). *Clin Infect Dis* **75**,
501 e630-e644 (2022).
502 5. L. Wieske *et al.*, Humoral responses after second and third SARS-CoV-2 vaccination in
503 patients with immune-mediated inflammatory disorders on immunosuppressants: a
504 cohort study. *Lancet Rheumatol* **4**, e338-e350 (2022).
505 6. J. D. Kelly *et al.*, Incidence of Severe COVID-19 Illness Following Vaccination and
506 Booster With BNT162b2, mRNA-1273, and Ad26.COV2.S Vaccines. *JAMA* **328**, 1427-
507 1437 (2022).
508 7. U. Agrawal *et al.*, Severe COVID-19 outcomes after full vaccination of primary schedule
509 and initial boosters: pooled analysis of national prospective cohort studies of 30 million
510 individuals in England, Northern Ireland, Scotland, and Wales. *Lancet* **400**, 1305-1320
511 (2022).
512 8. D. Planas *et al.*, Reduced sensitivity of SARS-CoV-2 variant Delta to antibody
513 neutralization. *Nature* **596**, 276-280 (2021).
514 9. M. Hoffmann *et al.*, SARS-CoV-2 variant B.1.617 is resistant to bamlanivimab and
515 evades antibodies induced by infection and vaccination. *Cell Reports* **36**, (2021).
516 10. Q. Wang *et al.*, Antibody evasion by SARS-CoV-2 Omicron subvariants BA.2.12.1, BA.4
517 and BA.5. *Nature* **608**, 603-608 (2022).
518 11. S. Weigang *et al.*, Within-host evolution of SARS-CoV-2 in an immunosuppressed
519 COVID-19 patient as a source of immune escape variants. *Nat Commun* **12**, 6405
520 (2021).
521 12. S. Cele *et al.*, SARS-CoV-2 prolonged infection during advanced HIV disease evolves
522 extensive immune escape. *Cell Host Microbe* **30**, 154-162 e155 (2022).
523 13. B. Choi *et al.*, Persistence and Evolution of SARS-CoV-2 in an Immunocompromised
524 Host. *N Engl J Med* **383**, 2291-2293 (2020).

525 14. M. K. Hensley *et al.*, Intractable Coronavirus Disease 2019 (COVID-19) and Prolonged
526 Severe Acute Respiratory Syndrome Coronavirus 2 (SARS-CoV-2) Replication in a
527 Chimeric Antigen Receptor-Modified T-Cell Therapy Recipient: A Case Study. *Clin Infect*
528 *Dis* **73**, e815-e821 (2021).
529 15. S. Harari *et al.*, Drivers of adaptive evolution during chronic SARS-CoV-2 infections. *Nat*
530 *Med* **28**, 1501-1508 (2022).
531 16. M. C. Choudhary, C. R. Crain, X. Qiu, W. Hanage, J. Z. Li, Severe Acute Respiratory
532 Syndrome Coronavirus 2 (SARS-CoV-2) Sequence Characteristics of Coronavirus
533 Disease 2019 (COVID-19) Persistence and Reinfection. *Clin Infect Dis* **74**, 237-245
534 (2022).
535 17. J. Boucau *et al.*, Duration of Shedding of Culturable Virus in SARS-CoV-2 Omicron
536 (BA.1) Infection. *N Engl J Med* **387**, 275-277 (2022).
537 18. M. S. Seaman *et al.*, Vaccine breakthrough infection leads to distinct profiles of
538 neutralizing antibody responses by SARS-CoV-2 variant. *JCI Insight* **7**, (2022).
539 19. M. J. Siedner *et al.*, Duration of viral shedding and culture positivity with postvaccination
540 SARS-CoV-2 delta variant infections. *JCI Insight* **7**, (2022).
541 20. V. A. Avanzato *et al.*, Case Study: Prolonged Infectious SARS-CoV-2 Shedding from an
542 Asymptomatic Immunocompromised Individual with Cancer. *Cell* **183**, 1901-1912.e1909
543 (2020).
544 21. C. Chaguza *et al.*, Accelerated SARS-CoV-2 intrahost evolution leading to distinct
545 genotypes during chronic infection. *Cell Rep Med* **4**, 100943 (2023).
546 22. B. Bailly *et al.*, Persistent Coronavirus Disease 2019 (COVID-19) in an
547 Immunocompromised Host Treated by Severe Acute Respiratory Syndrome Coronavirus
548 2 (SARS-CoV-2)-Specific Monoclonal Antibodies. *Clin Infect Dis* **74**, 1706-1707 (2022).
549 23. A. Truffot *et al.*, SARS-CoV-2 Variants in Immunocompromised Patient Given Antibody
550 Monotherapy. *Emerg Infect Dis* **27**, 2725-2728 (2021).
551 24. A. Gupta *et al.*, Host immunological responses facilitate development of SARS-CoV-2
552 mutations in patients receiving monoclonal antibody treatments. *J Clin Invest* **133**,
553 (2023).
554 25. J. H. Baang *et al.*, Prolonged Severe Acute Respiratory Syndrome Coronavirus 2
555 Replication in an Immunocompromised Patient. *J Infect Dis* **223**, 23-27 (2021).
556 26. Y. Bronstein *et al.*, Evolution of spike mutations following antibody treatment in two
557 immunocompromised patients with persistent COVID-19 infection. *J Med Virol* **94**, 1241-
558 1245 (2022).

559 27. A. S. Gonzalez-Reiche *et al.*, Sequential intrahost evolution and onward transmission of
560 SARS-CoV-2 variants. *Nat Commun* **14**, 3235 (2023).
561 28. M. C. Choudhary *et al.*, Emergence of SARS-CoV-2 escape mutations during
562 Bamlanivimab therapy in a phase II randomized clinical trial. *Nat Microbiol* **7**, 1906-1917
563 (2022).
564 29. S. A. Kemp *et al.*, SARS-CoV-2 evolution during treatment of chronic infection. *Nature*
565 **592**, 277-282 (2021).
566 30. S. A. Apostolidis *et al.*, Cellular and humoral immune responses following SARS-CoV-2
567 mRNA vaccination in patients with multiple sclerosis on anti-CD20 therapy. *Nat Med* **27**,
568 1990-2001 (2021).
569 31. V. Dioverti, S. Salto-Alejandre, G. Haidar, Immunocompromised Patients with Protracted
570 COVID-19: a Review of "Long Persisters". *Curr Transplant Rep*, 1-10 (2022).
571 32. V. Nussenblatt *et al.*, Yearlong COVID-19 Infection Reveals Within-Host Evolution of
572 SARS-CoV-2 in a Patient With B-Cell Depletion. *J Infect Dis* **225**, 1118-1123 (2022).
573 33. T. Aydillo *et al.*, Shedding of Viable SARS-CoV-2 after Immunosuppressive Therapy for
574 Cancer. *N Engl J Med* **383**, 2586-2588 (2020).
575 34. S. Gandhi *et al.*, De novo emergence of a remdesivir resistance mutation during
576 treatment of persistent SARS-CoV-2 infection in an immunocompromised patient: a case
577 report. *Nat Commun* **13**, 1547 (2022).
578 35. C. L. Gordon *et al.*, Defective Severe Acute Respiratory Syndrome Coronavirus 2
579 Immune Responses in an Immunocompromised Individual With Prolonged Viral
580 Replication. *Open Forum Infect Dis* **8**, ofab359 (2021).
581 36. I. Monrad *et al.*, Persistent Severe Acute Respiratory Syndrome Coronavirus 2 Infection
582 in Immunocompromised Host Displaying Treatment Induced Viral Evolution. *Open*
583 *Forum Infect Dis* **8**, ofab295 (2021).
584 37. K. M. Braun *et al.*, Acute SARS-CoV-2 infections harbor limited within-host diversity and
585 transmit via tight transmission bottlenecks. *PLoS Pathog* **17**, e1009849 (2021).
586 38. K. K. K. Ko *et al.*, Emergence of SARS-CoV-2 Spike Mutations during Prolonged
587 Infection in Immunocompromised Hosts. *Microbiol Spectr* **10**, e0079122 (2022).
588 39. K. A. Lythgoe *et al.*, SARS-CoV-2 within-host diversity and transmission. *Science* **372**,
589 (2021).
590 40. A. L. Valesano *et al.*, Temporal dynamics of SARS-CoV-2 mutation accumulation within
591 and across infected hosts. *PLoS Pathog* **17**, e1009499 (2021).

592 41. A. Soresina *et al.*, Two X-linked agammaglobulinemia patients develop pneumonia as
593 COVID-19 manifestation but recover. *Pediatr Allergy Immunol* **31**, 565-569 (2020).
594 42. T. Dangi *et al.*, Improved control of SARS-CoV-2 by treatment with nucleocapsid-specific
595 monoclonal antibody. *J Clin Invest*, e162282 [Online ahead of print] (2022).
596 43. R. Kundu *et al.*, Cross-reactive memory T cells associate with protection against SARS-
597 CoV-2 infection in COVID-19 contacts. *Nat Commun* **13**, 80 (2022).
598 44. K. Maneikis *et al.*, Immunogenicity of the BNT162b2 COVID-19 mRNA vaccine and early
599 clinical outcomes in patients with haematological malignancies in Lithuania: a national
600 prospective cohort study. *The Lancet Haematology* **8**, e583-e592 (2021).
601 45. J. Fajnzylber *et al.*, SARS-CoV-2 viral load is associated with increased disease severity
602 and mortality. *Nat Commun* **11**, 5493 (2020).
603 46. A. Nathan *et al.*, Structure-guided T cell vaccine design for SARS-CoV-2 variants and
604 sarbecoviruses. *Cell* **184**, 4401-4413.e4410 (2021).
605 47. P. L. Tzou, K. Tao, S. L. K. Pond, R. W. Shafer, Coronavirus Resistance Database
606 (CoV-RDB): SARS-CoV-2 susceptibility to monoclonal antibodies, convalescent plasma,
607 and plasma from vaccinated persons. *PLoS One* **17**, e0261045 (2022).
608 48. J. Z. Li *et al.*, Impact of pre-existing drug resistance on risk of virological failure in South
609 Africa. *J Antimicrob Chemother* **76**, 1558-1563 (2021).
610 49. I. Aksamentov, C. Roemer, E. B. Hodcroft, R. A. Neher, Nextclade: clade assignment,
611 mutation calling andquality control for viral genomes. *The Journal of Open Source*
612 *Software* **6**, 3773 (2021).
613

614

615 ## Figure Legends

616 **Figure 1. Kinetics of SARS-CoV-2 viral RNA and culturable virus among different**
617 **immunocompromised groups.** **a**, Upper respiratory viral load decay. Lower level of
618 quantification (LLOQ) is 10 copies/ml. **b**, Kaplan-Meier estimates of upper respiratory viral
619 clearance (viral load below LLOQ). **c**, Upper respiratory culturable virus dynamics (50% Tissue
620 Culture Infectious Dose [$TCID_{50}$)). **d**, Kaplan-Meier estimates of upper respiratory culturable
621 virus clearance.

622

623 **Figure 2. SARS-CoV-2 intra-host mutations among different immunocompromise groups.**
624 **a,** Number of intra-host single-nucleotide variants (iSNVs) among severe (S-HT in red and S-A
625 in green), non-severe immunocompromised and non-immunocompromised (None) groups. **b,**
626 Nucleotide average pairwise distance (APD) among severe (S-HT in red and S-A in green),
627 non-severe immunocompromised (NS) and non-immunocompromised (None) groups. **c**,
628 Participants with any nucleotide changes during follow-up. **d**, Heat map showing distribution of
629 Spike polymorphisms from participants receiving mAb treatment. Each row represents one
630 participant, while x axis shows amino acid positions in the Spike gene. Different domains of
631 Spike are shown at the top. Colors indicate frequency of polymorphisms, with blue indicating the
632 lowest value and red indicating the highest value in the scale. Participants in different study
633 groups are separated by a red horizontal line. **e**, Proportion of mAb resistance emergence
634 amongst those treated with mAbs, categorized by those with severe or non-severe/no
635 immunosuppression. Comparison of iSNV and APD between groups were done using using
636 Dunn's test with Benjamini-Hochberg P value adjustment. Fisher's exact test was used to
637 calculate significance between participants with and without viral evolution and further, in
638 participants with and without mAb treatment specific resistance mutations. Only significant P
639 values are shown. NTD, N-terminal domain; RBD, receptor binding domain; RBM, receptor
640 binding motif; S1, subunit 1; S2, subunit 2.

641

642 **Figure 3. Neutralizing antibody (nAb) and Nucleocapsid binding antibody levels among**
643 **different immunocompromised groups. a**, nAb levels (50% inhibitory dilution [ID_{50}]) against
644 ancestral Spike protein. **b**, nAb levels against variant-specific Spike protein. **c** and **d**,
645 Longitudinal trajectory of nAb in different immunocompromise groups, including (**c**) or excluding
646 (**d**) monoclonal antibody use. **e**, binding antibody levels against Nucleocapsid protein. **f**,
647 Longitudinal trajectory of binding antibody in different immunocompromise groups. Comparison
648 between different immunocompromise groups at the same time point was performed using
649 Dunn's test with Benjamini-Hochberg P value adjustment. Comparison of longitudinal antibody
650 changes for participants with two blood draws was performed using the pairwise Wilcoxon rank
651 sum test with Benjamini-Hochberg P value adjustment. Only significant P values were shown.
652 Tukey boxplot was used to summarize antibody levels. Generalized additive model was used to
653 evaluate the trend of antibody development with 95% confidence intervals in the shaded area.
654 Lines between two timepoints indicate the same participants with two blood draws. S-HT,
655 severe hematologic-oncology/transplant; S-A, severe autoimmune/B-cell deficient; NS, non-
656 severe. Severe group included both S-HT and S-A as they had comparable antibody levels at
657 multiple time points.

658

659 **Figure 4. Spike-specific T levels among different immunocompromised groups. a**,
660 enzyme-linked immunosorbent spot (ELIspot) assays using peptide pools derived from
661 ancestral and variant-specific Spike protein. **b, c**, $CD4^+$ T cell (b) and $CD8^+$ T cell proliferation
662 (c) upon stimulation of ancestral- and variant-specific Spike peptide pools. **d**, Longitudinal
663 trajectory of Spike-specific T levels in different immunocompromise groups. Comparison
664 between different immunocompromise groups at the same time point was performed using
665 Dunn's test with Benjamini-Hochberg P value adjustment. Comparison of longitudinal antibody
666 changes for participants with two blood draws was performed using the pairwise Wilcoxon rank

sum test with Benjamini-Hochberg P value adjustment. Only significant P values were shown. Tukey boxplot was used to summarize antibody levels. Generalized additive model was used to evaluate the trend of antibody development with 95% confidence intervals in the shade area. Lines between two timepoints indicate the same participants with two blood draws.

Table 1. Demographic and clinical information.

	Immunocompromised (N=56)	Non-Immunocompromised (N=184)	Total (N=240)	P value
Sex, n (%)				0.2
Female	32 (57.1%)	126 (68.5%)	158 (65.8%)	
Male	24 (42.9%)	58 (31.5%)	82 (34.2%)	
Age, Median (Q1, Q3)	55 (45, 67)	46 (33, 59)	49 (34-60)	0.001
Race, n (%)				0.8
Asian	1 (1.8)	10 (5.4)	11 (4.6)	
Black or AA	5 (8.9)	19 (10.3)	24 (10.0)	
Other/Unknown	5 (8.9)	16 (8.7)	21 (8.8)	
White	45 (80.4)	139 (75.5)	184 (76.7)	
Ethnicity				0.5
Hispanic or Latino	5 (8.9)	17 (9.2)	22 (9.2)	
Not Hispanic or Latino	47 (83.9)	143 (77.7)	190 (79.2)	
Other/Unknown	4 (7.1)	24 (13.0)	28 (11.7)	
Inpatient, n (%)	7 (12.5)	8 (4.3)	15 (6.2)	0.051
Number of vaccinations, median number, (Q1, Q3)	3 (3-4)	3 (2-3)	3 (2-4)	<0.001
mAb use, n (%)	24* (42.9)	10 (5.4)	34 (14.2)	<0.001
Antiviral use, n (%)	40 (71.4)	57 (31.0)	97 (40.4)	<0.001
Immunocompromise group, n (%)				<0.001
S-HT	12 (21.4)	0 (0.0)	12 (5.0)	
S-A	13 (23.2)	0 (0.0)	13 (5.4)	
NS	31 (55.4)	0 (0.0)	31 (12.9)	
None	0 (0.0)	184 (100.0)	184 (76.7)	
Symptom duration, median days** (Q1, Q3)	5 (4, 7)	4 (3, 6)	4 (3, 6)	0.04
Variant***				<0.001
Delta	3 (5.4)	43 (23.4)	46 (19.2)	
Omicron	48 (85.7)	137 (74.5)	185 (77.1)	
Other/Unknown	5 (8.9)	4 (2.2)	9 (3.8)	

Q1 and Q3, quartile 1 and quartile 3; AA, African American; mAb, monoclonal antibody; S-HT, severe with malignant hematology or transplant history; S-A, severe autoimmune/B-cell deficient; NS, non-severe immunocompromising condition.

*, four participants received Mab after blood draws.

**, Symptom duration indicates the duration between symptom onset (patient report or first positive test if asymptomatic screening) and first nasal swab collected by the study group.

***, Variant information was obtained by either Spike or whole genome sequencing or by epidemiological information (time period when the participant was infected).

Table 2. Association between immunocompromise groups and SARS-CoV-2 viral decay.

Hazard ratio for SARS-CoV-2 viral RNA clearance				
Group	HR (95% CI)	P	aHR (95% CI)	P
None (Reference)				
S-HT	0.22 (0.09-0.52)	0.0005	0.32 (0.12-0.83)	0.02
S-A	0.64 (0.34-1.22)	0.2	0.74 (0.33-1.64)	0.5
NS	0.82 (0.54-1.24)	0.4	0.92 (0.58-1.46)	0.7
Hazard ratio for SARS-CoV-2 culturable virus clearance				
Group	HR (95% CI)	P	aHR (95% CI)	P
None (Reference)				
S-HT	0.23 (0.11-0.48)	8.7E-5	0.27 (0.12-0.63)	0.002
S-A	0.54 (0.28-1.03)	0.06	0.53 (0.26-1.11)	0.09
NS	1.12 (0.76-1.66)	0.6	1.35 (0.89-2.06)	0.2

HR, hazard ratio; aHR, adjusted hazard ratio; CI, confidence interval.

Age, sex at birth, race, ethnicity, number of vaccinations, monoclonal use, and antiviral use were adjusted for in the multivariate models.

Figure 1

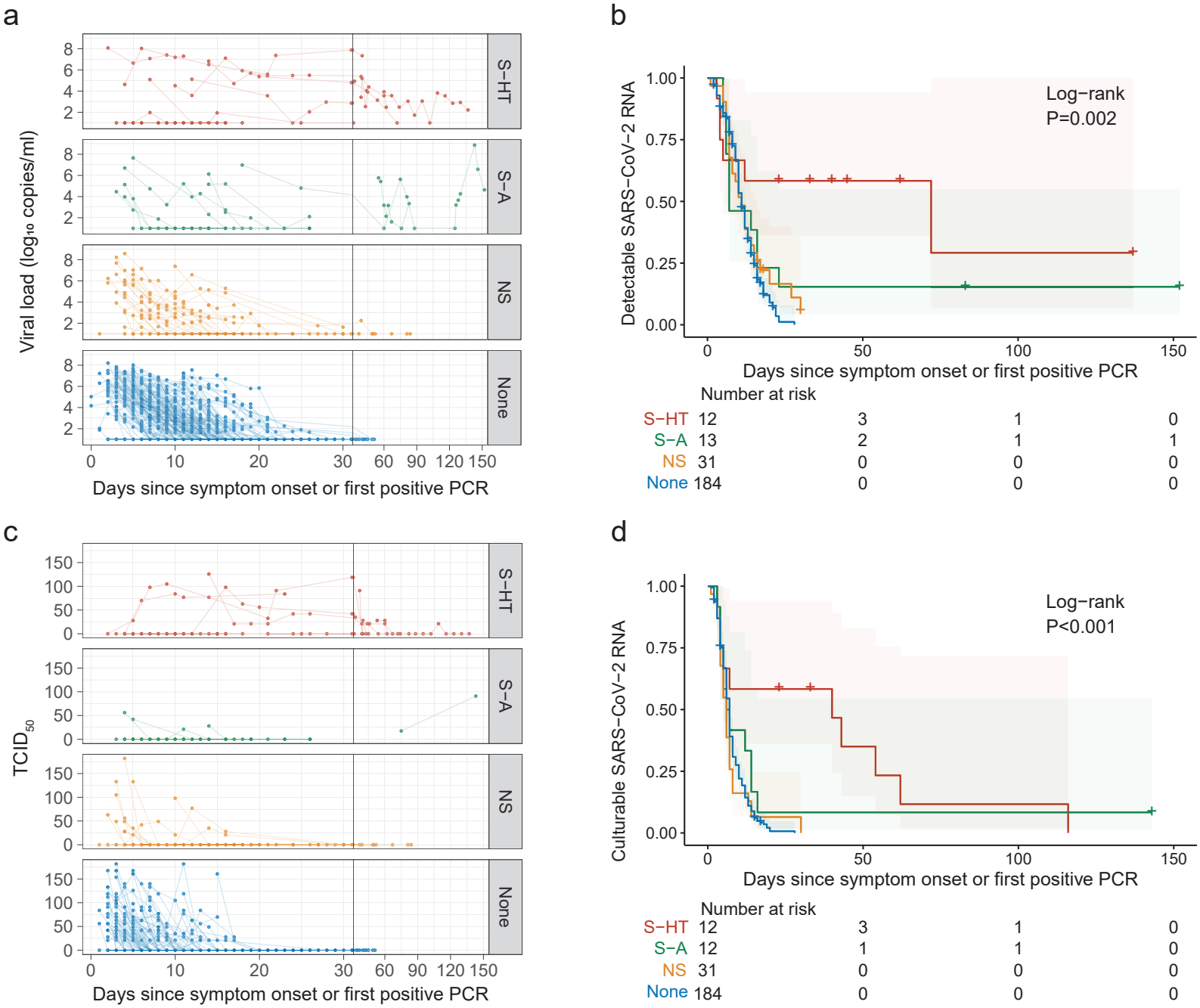
a
Viral load (log10 copies/ml)
S−HT
S−A
NS
None
Days since symptom onset or first positive PCR
b
Detectable SARS−CoV−2 RNA
Log−rank
P=0.002
Days since symptom onset or first positive PCR
Number at risk
S−HT 12 3 1 0
S−A 13 2 1 1
NS 31 0 0 0
None 184 0 0 0
c
TCID50
S−HT
S−A
NS
None
Days since symptom onset or first positive PCR
d
Culturable SARS−CoV−2 RNA
Log−rank
P<0.001
Days since symptom onset or first positive PCR
Number at risk
S−HT 12 3 1 0
S−A 12 1 1 0
NS 31 0 0 0
None 184 0 0 0

Figure 2

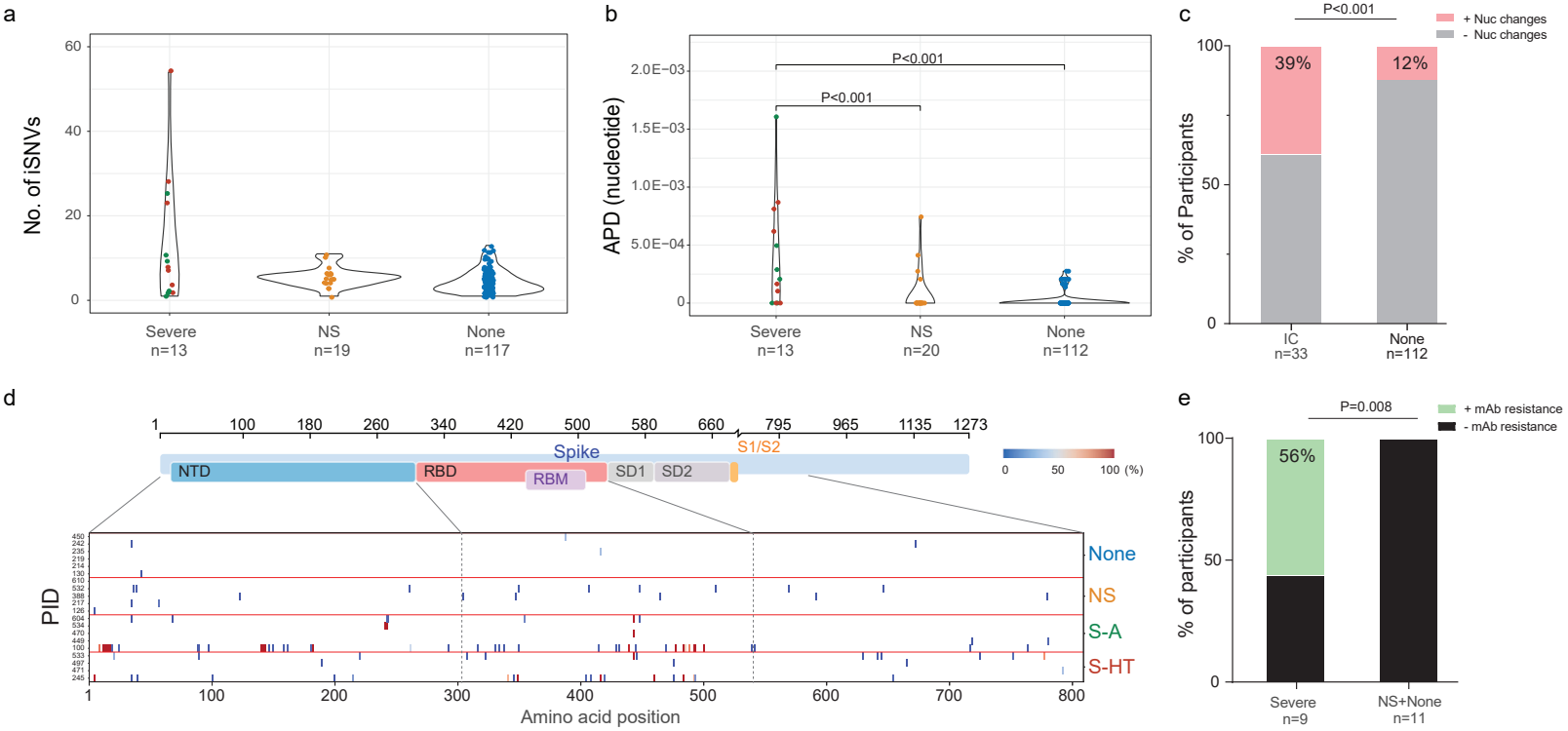
a
No. of iSNVs
Severe n=13
NS n=19
None n=117
b
APD (nucleotide)
P<0.001
P<0.001
Severe n=13
NS n=20
None n=112
c
P<0.001
+ Nuc changes
- Nuc changes
% of Participants
39%
12%
IC n=33
None n=112
d
Spike
NTD
RBD
RBM
SD1
SD2
S1/S2
PID
None
NS
S-A
S-HT
Amino acid position
e
P=0.008
+ mAb resistance
- mAb resistance
% of participants
56%
Severe n=9
NS+None n=11

Figure 3

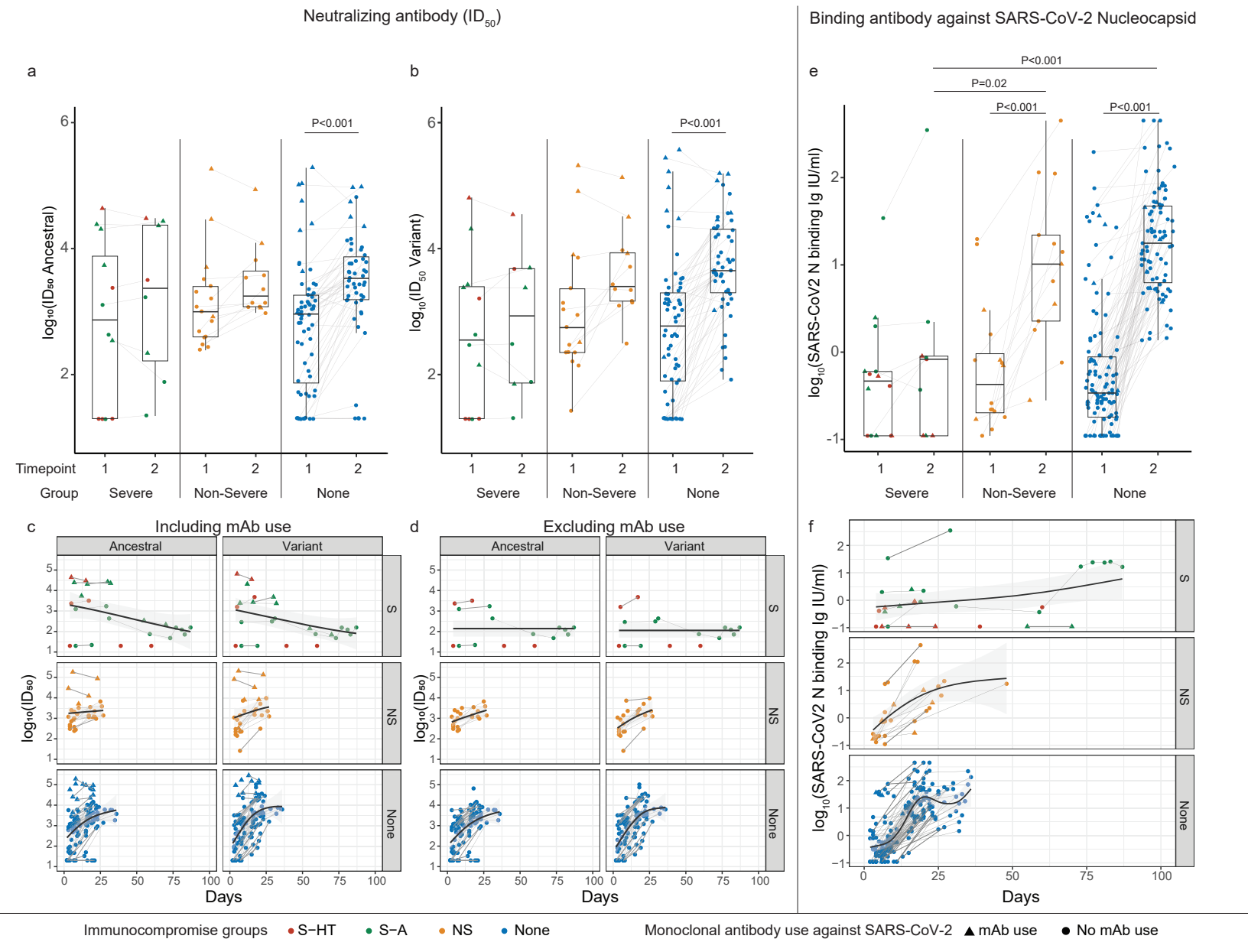
Neutralizing antibody (ID50)
Binding antibody against SARS-CoV-2 Nucleocapsid
a
b
e
P<0.001
P=0.02
log10(ID50 Ancestral)
log10(ID50 Variant)
log10(SARS-CoV2 N binding Ig IU/ml)
Timepoint
Group
Severe
Non-Severe
None
c
d
f
Including mAb use
Excluding mAb use
Ancestral
Variant
S
NS
Days
Immunocompromise groups
S−HT
S−A
NS
None
Monoclonal antibody use against SARS-CoV-2
mAb use
No mAb use

Figure 4

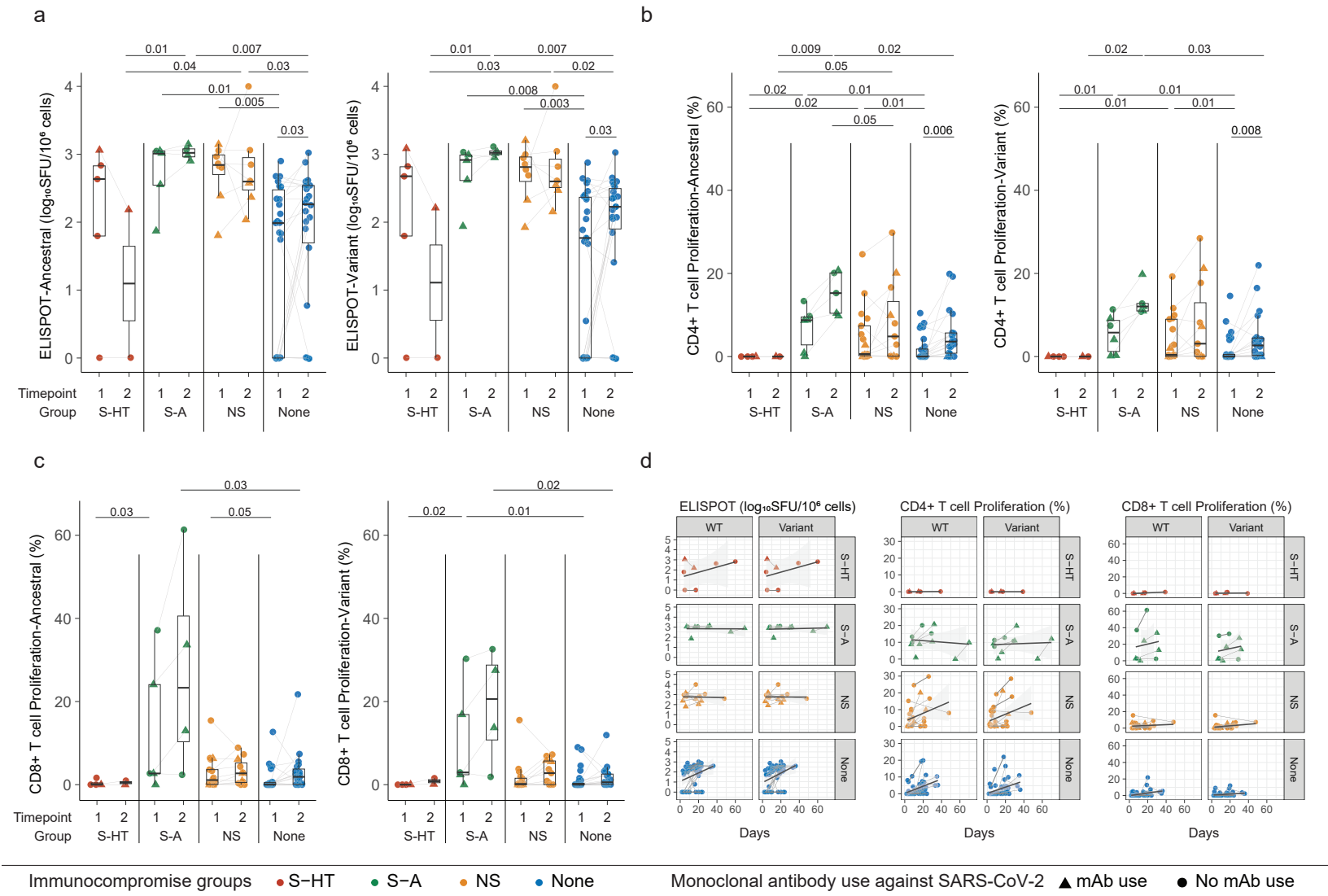
a
b
c
d
ELISPOT-Ancestral (log₁₀SFU/10⁶ cells)
ELISPOT-Variant (log₁₀SFU/10⁶ cells)
CD4+ T cell Proliferation-Ancestral (%)
CD4+ T cell Proliferation-Variant (%)
CD8+ T cell Proliferation-Ancestral (%)
CD8+ T cell Proliferation-Variant (%)
Timepoint
Group
S-HT
S-A
NS
None
ELISPOT (log₁₀SFU/10⁶ cells)
CD4+ T cell Proliferation (%)
CD8+ T cell Proliferation (%)
WT
Variant
Days
Immunocompromise groups
S−HT
S−A
NS
None
Monoclonal antibody use against SARS-CoV-2
mAb use
No mAb use

Supplementary Materials

Supplementary Methods 2
T cell proliferation staining panels 2
Generalized estimating equation (GEE) 2
Supplementary Tables 3
Supplementary Table 1. Categorization for immunocompromising conditions 3
Supplementary Table 2. Diagnoses for immunocompromised participants and categorization. 4
Supplementary Table 3. Monoclonal antibody use. 6
Supplementary Figures 7
Supplementary Figure 1. Detectable SARS-CoV-2 viral RNA (a) and culturable SARS-CoV-2 virus (b) beyond 30 days after symptom onset or first positive PCR/antigen tests, supplemental to Fig. 1. 7
Supplementary Figure 2. SARS-CoV-2 mutations among different immunocompromised groups, supplementary to Fig. 2. 8
Supplementary Figure 3. Severe immunocompromise is associated with lower neutralizing antibody levels, supplemental to Fig. 3. 9
Supplementary Figure 4. Representative T cell proliferation assay gating scheme, supplementary to Fig. 4. 10
Supplementary Figure 5. Distribution of duration between symptom onset or first positive PCR and blood draws. 11
References 12

Supplementary Methods

T cell proliferation staining panels

For PBMCs stained with carboxyfluorescein succinimidyl ester (CFSE; Life Technologies), cells were then washed and stained with anti-CD3 PE-Cy7 (clone SK7; BioLegend), anti-CD8 APC (clone SK1; BioLegend), anti-CD4 BV711 (clone RPA-T4; BioLegend), and LIVE/DEAD violet viability dye (Life Technologies).

For PBMCs stained with Cell Trace Far Red Proliferation Dye (CTFR, Invitrogen), cells were then washed and stained with anti-CD3 APC-Cy7 (clone UCHT1; BioLegend), anti-CD8 BV605 (clone SK1; BioLegend), anti-CD4 PE-Cy7 (clone OKT4; BioLegend), and LIVE/DEAD violet viability dye (Life Technologies).

Generalized estimating equation (GEE)

GEE was performed using “geepack” package (version 1.3.9) in R[1]. In the GEE model, family was set as “gaussian”, and the correlation structure (“corstr”) was set as “independence”. Quasi Information Criterion (QIC) was used to compare models using “independence”, “exchangeable” and “ar1” and the one with “independence” had the lowest QIC. Monoclonal antibody (Mab) use, weeks since symptom onset or first positive PCR, numbers of vaccinations before enrollment, sex, and age were adjusted for in these models. Logarithm base 10 of the neutralizing antibody levels were treated as dependent variables and other variables as independent. Coefficients for all the independent variables were then transformed to the power of 10 and was shown in this figure as fold-change compared to reference group.

Supplementary Tables

Supplementary Table 1. Categorization for immunocompromising conditions.

Non-Severe (NS)		• Autoimmune disease, receiving immunosuppressants that are not B cell/plasma cell targeted therapy within 12 months of study entry • Solid malignant tumor on treatment (excluding those who underwent resection and were considered in remission after resection) • Corticosteroid use equivalent to Prednisone >20mg daily for at least 14 consecutive days within 30 days prior to study entry • HIV infection with CD4 cell count >200 cells/mm^3
Severe	Severe- Hematological malignancy/Transplant (S-HT)	• Solid organ transplant (SOT) • Hematopoietic stem cell transplant (HSCT) • Lymphoma, leukemia • Immune-Related Adverse Event (irAE) on multiple immunosuppressants targeting different pathways
	Severe- Autoimmune and other B cell deficiency (S-A)	• Autoimmune disease receiving B cell targeted therapy within 12 months of study entry • Congenital or late onset B cell deficiency (e.g. Common Variable Immunodeficiency)

Supplementary Table 2. Diagnoses for immunocompromised participants and categorization.

ID	Diagnosis	Immunosuppressants/Treatment	Group
100	Antiphospholipid syndrome	Prednisone, eculizumab, rituximab, cyclophosphamide	S-A
101	Heart and kidney transplant	Everolimus, Prednisone 5mg daily, Tacrolimus	S-HT
107	Rheumatoid arthritis	Tocilizumab	NS
113	Minimal change disease	Rituximab within 12 months of COVID-19	S-A
126	RA	Abatacept+ Prednisone 5mg daily	NS
217	RA	Methotrexate+ Prednisone 5mg daily	NS
240	Chronic myelogenous leukemia	Dasatinib	S-HT
245	Diffuse large B-cell lymphoma	Rituximab+Polatuzumab+Prednisone, CAR-T, Chemotherapy, Tocilizumab	S-HT
388	Adenocarcinoma of pancreas	Chemotherapy and radiation	NS
449	Granulomatosis with polyangiitis	Rituximab within 12 months of COVID-19	S-A
459	Immune Related Adverse Events, Metastatic Merkel cell carcinoma	Pembrolizumab, Tacrolimus, Prednisone, Mycophenolate	S-HT
470	Multiple sclerosis	Ocrelizumab within 12 months of COVID-19	S-A
471	Marginal zone lymphoma (CR)	Obinutuzumab+CHOP	S-HT
475	Multiple sclerosis	Rituximab within 12 months of COVID-19	S-A
497	Diffuse large B-cell lymphoma (CR), Hypogammaglobulinemia	Rituximab-CHOP	S-HT
531	Sarcoidosis	Infliximab	NS
532	Granulomatosis with polyangiitis	Mycophenolate	NS
533	Diffuse large B cell lymphoma, Hypogammaglobulinemia after CAR-T	CAR-T, Tocilizumab, Pembrolizumab, Rituximab, Corticosteroid	S-HT
534	RA, Sjogren's syndrome, Hypogammaglobulinemia; cryoglobulinemia	IVIG	S-A
547	RA	Tocilizumab+Methotrexate	NS
548	RA	Rituximab within 12 months of COVID-19+ Leflunomide	S-A
549	Bechet’s disease	Azathioprine	NS
550	RA	Methotrexate+ Hydroxychloroquine	NS
551	Psoriatic arthritis	Infliximab	NS
552	Seronegative spondyloarthropathy	Adalimumab+ Methotrexate	NS
557	RA, SLE	Methotrexate	NS
558	SLE	Belimumab	S-A
563	RA	Adalimumab	NS
564	Multiple myeloma	Daratumumab+ Dexamethasone	S-HT
569	SLE	Hydroxychloroquine+ Methylprednisolone daily 6mg	NS
573	Inflammatory arthritis	Adalimumab+ Hydroxychloroquine	NS

597	Giant cell arteritis, polymyalgia rheumatica	Tocilizumab+ Prednisone orally 5mg daily	NS
604	CVID	IVIG every 4 weeks	S-A
610	Ulcerative colitis	Infliximab	NS
658	RA	Tocilizumab	NS
678	RA	Tofacitinib	NS
687	SLE, RA	Hydroxychloroquine, methotrexate	NS
688	Mantle cell lymphoma	Zanubrutinib+Venetoclax; Last dose of Obinutuzumab within 12 months	S-HT
691	RA	Rituximab	S-A
708	Minimal change disease	Rituximab	S-A
716	RA	Methotrexate	NS
723	Multiple sclerosis, acquired hypogammaglobulinemia	IVIG every 4 weeks; Ocrelizumab within 12 months	S-A
725	RA	Infliximab, methotrexate, hydroxychloroquine	NS
735	Psoriatic arthritis	Adalimumab	NS
768	Ankylosing spondylitis	Secukinumab	NS
793	RA	Adalimumab, methotrexate	NS
805	Ulcerative colitis, inflammatory arthritis	Golimumab, methotrexate	NS
870	Mantle cell lymphoma	Bendamustine and rituximab within 12 months	S-HT
892	HIV infection	N/A, on antiretroviral therapy, CD4 cell count>200	NS
936	RA	Etanercept, hydroxychloroquine	NS
945	IgG4 related disease	Rituximab	S-A
946	Diffuse large B-cell lymphoma	R-CHOP	S-HT
952	Inflammatory arthritis	Adalimumab	NS
953	RA	Infliximab, methotrexate, prednisone 3mg	NS
965	Breast cancer	Trastuzumab deruxtecan within 12 months, then Olaparib	NS
982	Follicular lymphoma	Bendamustine, Obinutuzumab within 12 months	S-HT

S-HT, severe hematological oncology/Transplant; S-A, severe autoimmune disease/B-cell deficient; NS, non-severe immunocompromise; CAR-T, chimeric antigen receptor T-cell therapy; CR, complete remission; CHOP, cyclophosphamide, doxorubicin, vincristine, and prednisone; R-CHOP, Rituximab in combination with CHOP; RA, rheumatoid arthritis; SLE, systemic lupus erythematosus; CVID, common variable immunodeficiency

Supplementary Table 3. Monoclonal antibody use.

	S-HT (N=12)	S-A (N=13)	NS (N=31)	None (N=184)	Overall (N=240)
Bamlanivimab-Etesevimab	1	0	0	4	5
Casirivimab-Imdevimab	0	2[b]	2	5	9
Sotrovimab	4[a]	1	1	0	6
Bebtelovimab	3	2	2	1	8
Tixagevimab-Cilgavimab	5[c]	4	0	0	9

a, three participants received Sotrovimab after blood draws.

b, one participant received Casirivimab-Imdevimab after blood draws.

c, two participants received both Tixagevimab-Cilgavimab and Sotrovimab and one participant received both Tixagevimab-Cilgavimab and Bebtelovimab

Supplementary Figures

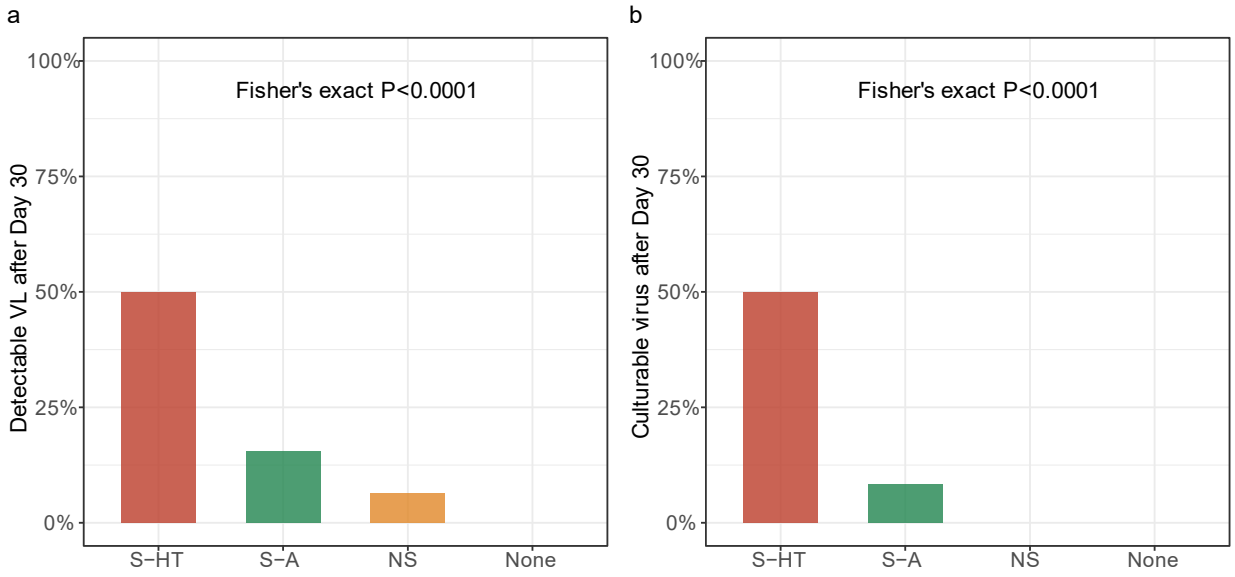

Supplementary Figure 1. Detectable SARS-CoV-2 viral RNA (a) and culturable SARS-CoV-2 virus (b) beyond 30 days after symptom onset or first positive PCR/antigen tests, supplemental to Fig. 1.

Fisher's exact test was used to calculate the P values.

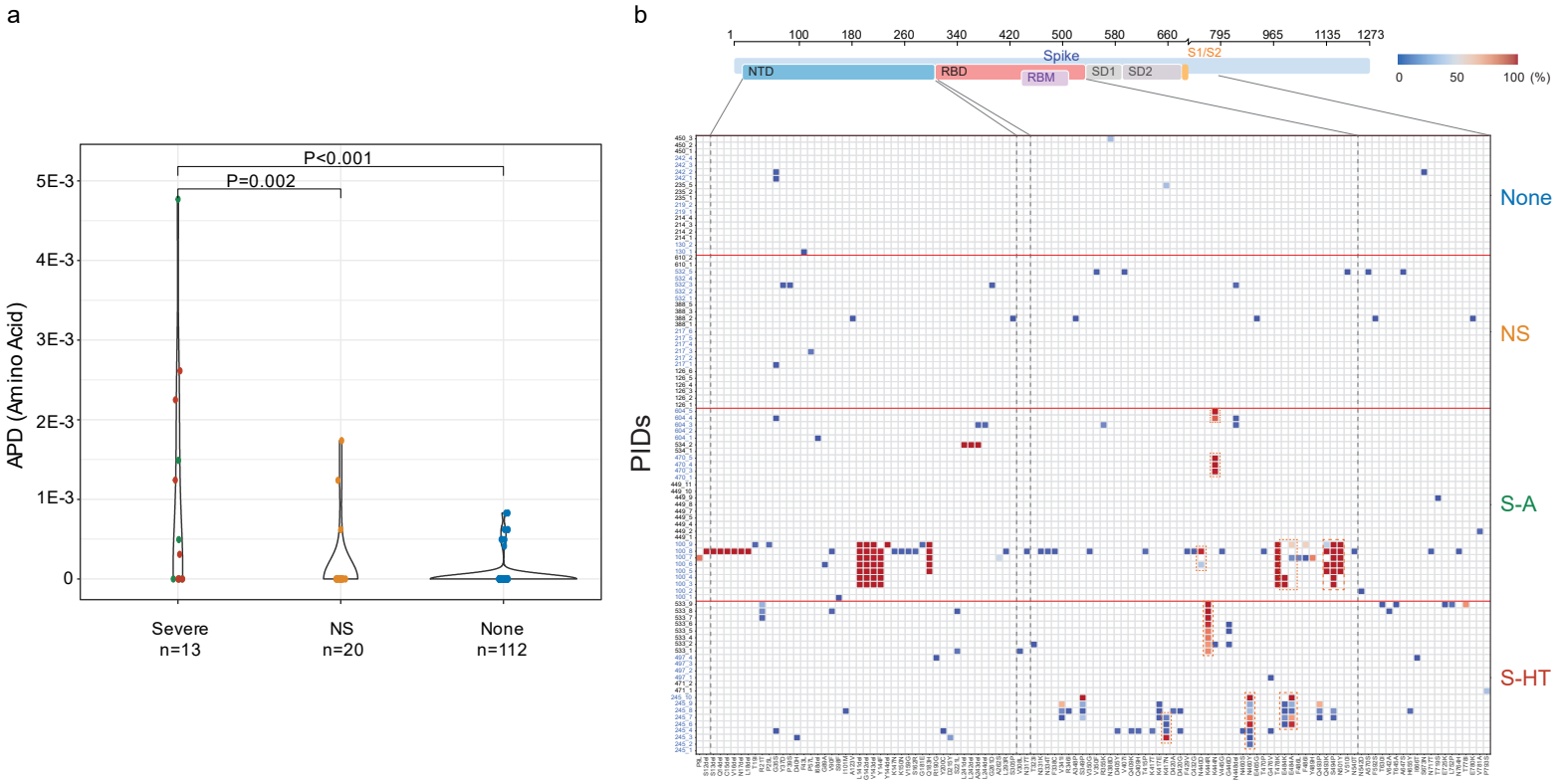

Supplementary Figure 2. SARS-CoV-2 mutations among different immunocompromised groups, supplementary to Fig. 2.

(a), SARS-CoV-2 intrahost mutations at the amino acid level among different immunocompromise groups. (b), Heat map showing distribution of Spike polymorphisms from participants receiving mAb treatment longitudinally. In the heatmap, y axis indicates participants' ID (PID) followed by sequential numbers of sample collection, while x axis shows amino acid positions in the Spike gene. Different domains of Spike are shown at the top. Colors indicate frequency of polymorphisms, with blue indicating the lowest value and red indicating the highest value in the scale. Participants in different study groups are separated by a red horizontal line. mAb resistance mutations are shown by red dotted box.

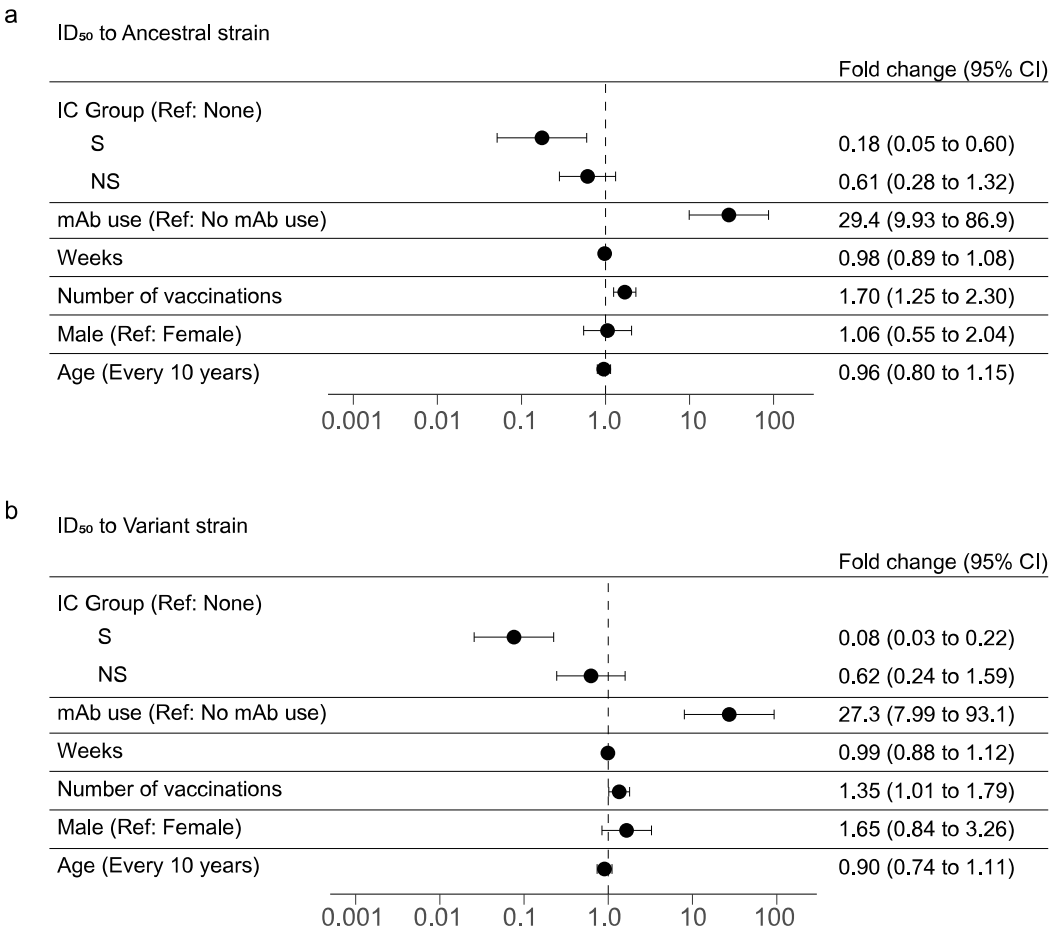

Supplementary Figure 3. Severe immunocompromise is associated with lower neutralizing antibody levels, supplemental to Fig. 3.

Generalized estimation equation to account for longitudinal repeated measurements was used to estimate the association between immunocompromise groups and neutralizing antibody levels against ancestral SARS-CoV-2 Spike protein (a) and variant-specific Spike protein (b). Monoclonal antibody (mAb) use, weeks since symptom onset or first positive PCR/antigen, numbers of vaccinations before enrollment, sex, and age were adjusted for in these models.

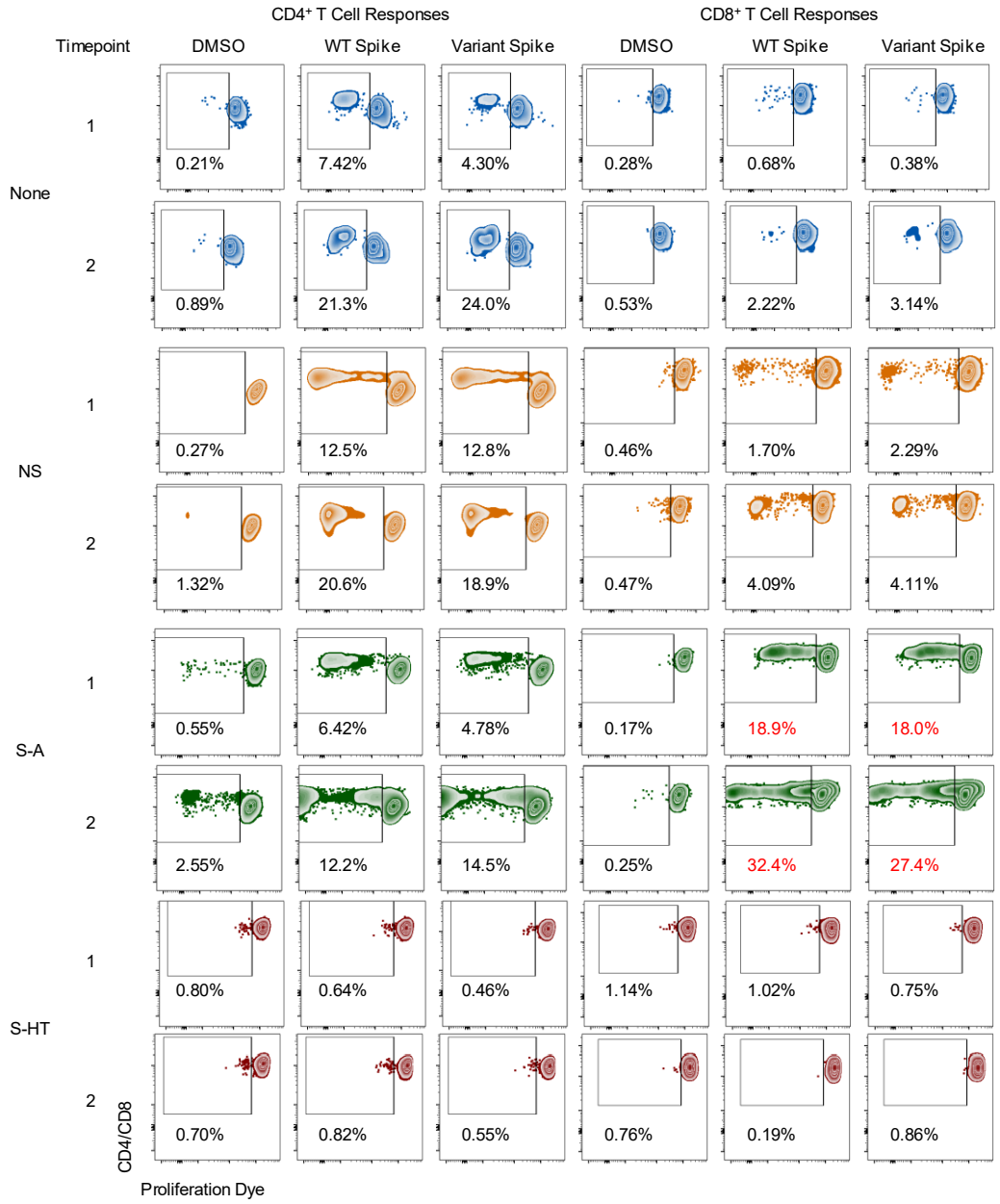

Supplementary Figure 4. Representative T cell proliferation assay gating scheme, supplementary to Fig. 4.

CD4+ and CD8+ T cell proliferation results from representative participants in each immunocompromise group are shown. Non-immunocompromised group, ID=261 (Omicron, BA.1); Non-severe group (NS), ID= 768 (Omicron, BF.5); Severe-autoimmune/B-cell deficient (S-A), ID=534 (Omicron, BA.2); Severe- hematological malignancy/transplant (S-HT), ID= 245 (Delta, B.1.617.2).

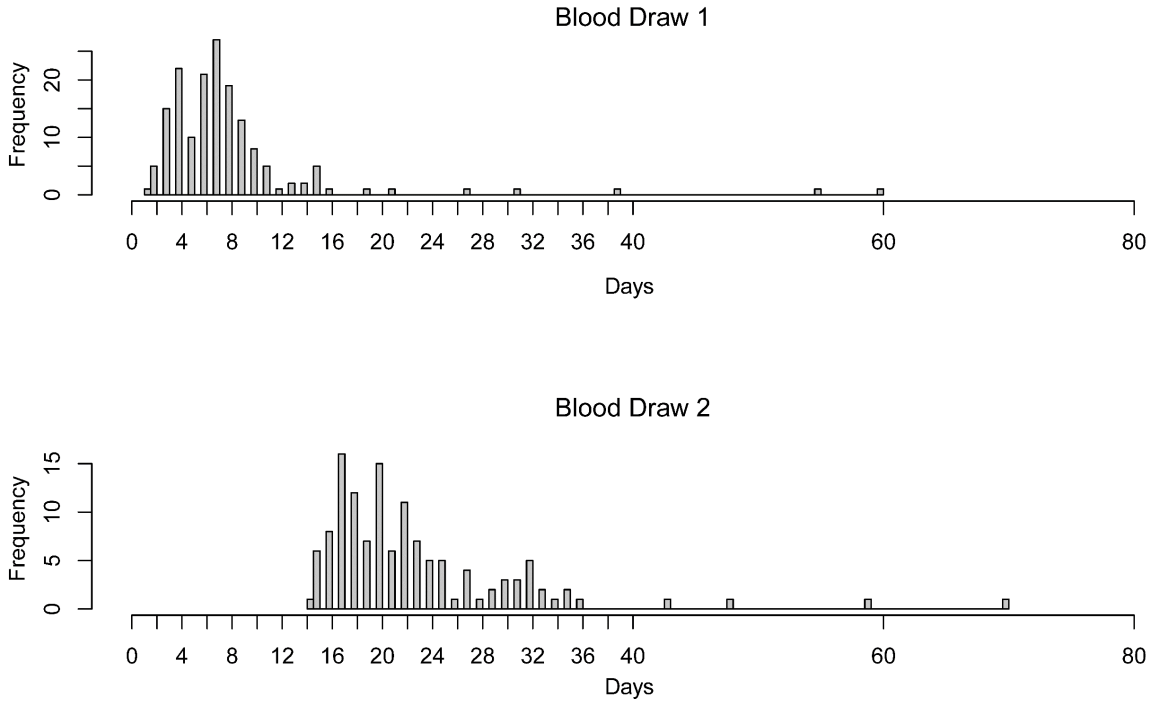

Supplementary Figure 5. Distribution of duration between symptom onset or first positive PCR and blood draws.

References

1. Højsgaard, S., Halekoh, U. & Yan, J. The R Package geepack for Generalized Estimating Equations. *Journal of Statistical Software* **15**, 1 - 11 (2005).